Journal of Thermal Analysis and Calorimetry, Vol. 65 (2001) 103–120

KINETIC MODELLING OF THE CONCENTRATIONS OF THE STABILIZER DPA AND SOME OF ITS CONSECUTIVE PRODUCTS AS FUNCTION OF TIME AND TEMPERATURE

M. A. Bohn[*]

Fraunhofer-Institut für Chemische Technologie (ICT), Postfach 1240,
D-76318 Pfinztal-Berghausen, Germany

(Received October 12, 2000; in revised form January 26, 2001)

Abstract

By kinetic modelling of the possible reactions of diphenylamine (DPA) and its nitrated consecutive products used to stabilize cellulose nitrate (CN), one can get reactivities for the nitrated DPA compounds for the situation inside a real CN formulation and therewith determine their stabilizing contribution. Concentration data of DPA and seven of its consecutive products have been determined by HPLC from isothermal ageing of a CN formulation at temperatures between 65 and 90°C for up to 344 days. A comparison between the modelling presented and modellings published in the literature using the steady-state approximation is made. The steady-state approximation oversimplifies the stabilizer reaction behaviour in a CN formulation. From the applied modelling the question about N–NO–DPA as a key intermediate can be answered.

Keywords: cellulose nitrate, DPA consecutive products, kinetic modelling, nitrocellulose, reactivity of reaction products, stabilizer diphenylamine

Introduction

Diphenylamine (DPA) is used to stabilize cellulose nitrate (CN), also widely named nitrocellulose (NC). DPA prevents the decomposition of CN by chemically bonding with the autocatalytically effective reaction products NO_2 and HNO_3 of the CN decomposition. Autocatalytic decomposition means that the decomposition of a reactant A forms at least one product B, which reacts with A in at least one further reaction and forms thereby at least one more B. The species NO_2, NO, N_2O_3, N_2O_4, HNO_2 and HNO_3 are connected by many reactions and, as an effective nitration species, the NO_2 radical is considererd. Electrophilic aromatic nitration by HNO_3 is not definitely exclused, but it seems unrealistic to assume that the conditions in a NC formulation

* E-mail: bo@ict.fhg.de

1418–2874/2001/ $ 5.00

Akadémiai Kiadó, Budapest
Kluwer Academic Publishers, Dordrecht

are as drastic as demanded for such a reaction type. The reaction of DPA with NO_2 forms consecutive products of DPA, which have a stabilizing effect too and are named secondary stabilizers. The important ones are N–NO–DPA, 2-NO_2–DPA, 4-NO_2–DPA and the dinitrated products. Figure 1 shows the chemical formulas of DPA and some of its products.

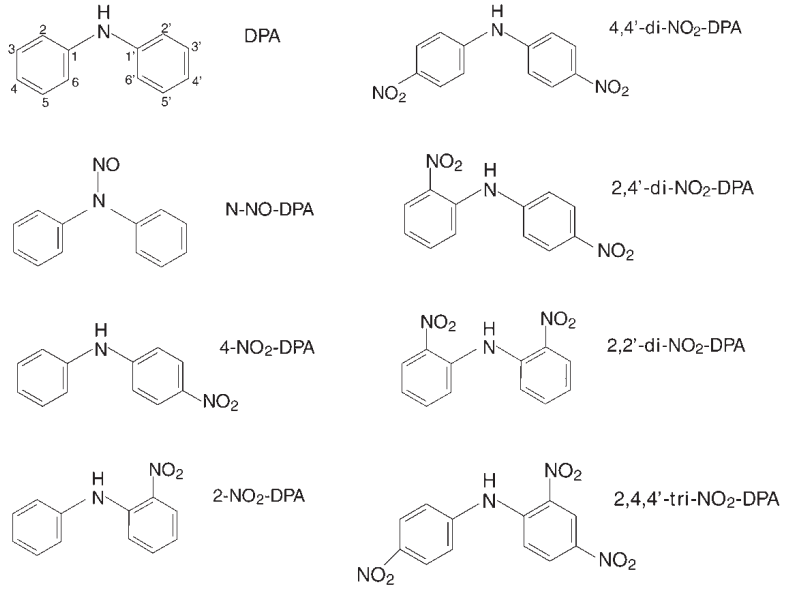

Fig. 1 Chemical formulas of diphenylamine (DPA) and of the considered DPA consecutive products. For DPA the ring numbering convention is shown

Considering only the consumption of the primary stabilizer DPA leads to a non-optimal use of the safe service time period and the reliable service time period of CN products. The safe service time period means the time period in which the NC product does not autoignite. The reliable service time period means the time period in which the functional properties remain within the tolerance limits. To improve the predicted service time periods, the appropriate stabilizing effects of the consecutive products must be considered. One, but probably the best, way to achieve this is by kinetic modelling of all the stabilizer reactions. For a CN formulation, an extensive determination by high performance liquid chromatography (HPLC) analysis was made of the concentrations of DPA and of its most important products as functions of time and temperature. The samples were aged isothermally in pyrex glass tubes closed with loosely inserted ground-in stoppers placed in aluminium block ovens with a temperature control maintained between ±0.5°C over long time periods. The temperatures were 65, 70, 75, 80, 85 and 90°C, and the storage times were up to 344 days. Figures 2 to 4 show examples of the data at 90, 85 and 65°C. In Fig. 2 the particle balance with regard to DPA can be seen also. The particle balance means that the con-

centration values of all measured consecutive products are transformed to mass% values of a corresponding pseudo-DPA and summed up together with the DPA concentrations. Ideally this particle balance should then stay at the start value at time zero. It decreases with time, probably because further DPA products are formed, see for example [5].

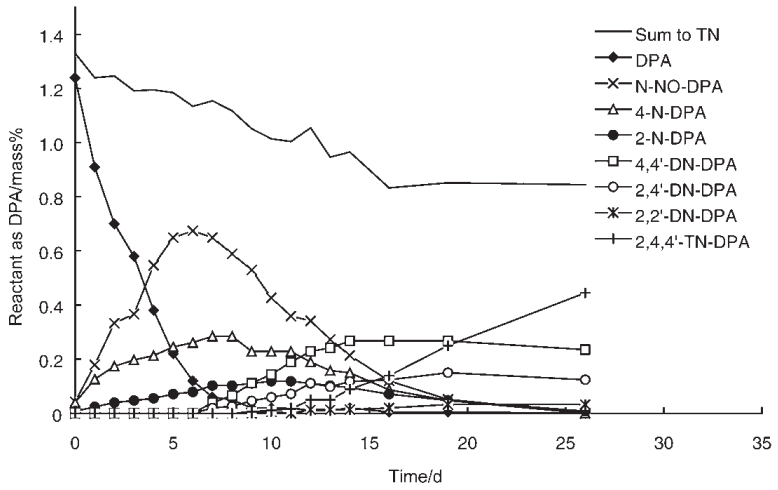

Fig. 2 Concentration data as functions of the ageing times of DPA and of the measured consecutive products at 90°C. For the particle balance of DPA the concentration data of all the measured DPA consecutive products are calculated as DPA concentrations in terms of mass% and summed up together with the DPA data

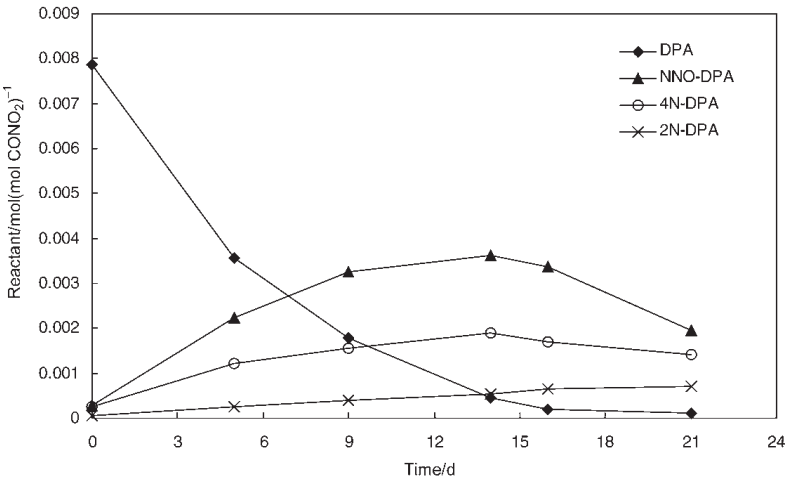

Fig. 3 Normalized concentration data of DPA, N–NO–DPA, 4-NO_2–DPA and 2-NO_2–DPA at 85°C as functions of ageing time

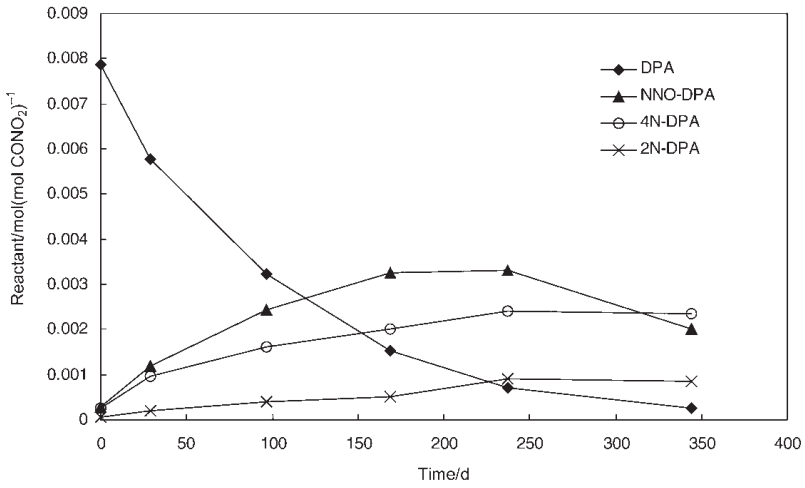

Fig. 4 Normalized concentration data of DPA, N–NO–DPA, 4-NO_2–DPA and 2-NO_2–DPA at 65°C as functions of ageing time

Modelling

Two main types of modellings are possible. The first uses the complete reaction scheme with explicit formulation of all the reactions with all reactants. The second simplifies the problem by applying the kinetic steady-state approximation for the autocatalytically effective product, assuming that the stabilizer keeps it at a constant concentration. In this section the first approach is used. The simplified modelling is discussed in section 'Discussion'. A homogenous kinetic description is used, because the production of such NC formulations is performed at temperatures much higher than the melting point of DPA at 55°C and the NC dough is thoroughly mixed. DPA is then well dispersed and the decomposition of the $CONO_2$ groups can be considered to occur statistically in time and space of the NC formulation, which means that the reaction behaviour is pseudo-homogenous.

First step modelling

In the first step only the primary stabilizer is considered in the reaction scheme. The conceptual base is that the primary stabilizer forms no consecutive products, or that the consecutive products have a much lower reactivity than the primary stabilizer. The corresponding reaction scheme is shown below as RS I-E, which is extended in comparison to the one given in [4]. It contains two reaction channels for the decomposition of the NC. One is the thermolysis of the $CONO_2$ group, which means a homolytic cleavage of the CO–NO_2 bond, in which two radicals are formed, with an activation energy of about 160 to 170 kJ mol^{-1} [1–3]. In [3], some compounds containing nitric acid ester groups have been investigated by adiabatic self-heating. The other channel is the hydrolysis of the $CONO_2$ group, which has an activation energy

of about 100 kJ mol^{-1} [2]. Thermolysis produces the NO_2 radical, which can attack the backbone of NC by oxidation and/or by H radical abstraction with HNO_2 formation. The NO_2 attack triggers further release of NO_2 by rearrangement reactions of the damaged NC backbone. Hydrolysis gives nitric acid, HNO_3, which catalyses the saponification of the ester group. Both products P_T and P_H react in different ways with NC and with the stabilizer. Because there are many reactions possible between NO_2, N_2O_3, N_2O_4, HNO_2, NO and HNO_3 , only one species is assumed in the reduced reaction scheme RS I as an autocatalytically effective product P, which reacts in one channel with NC. It is necessary to reduce the complexity of the reaction scheme because not enough information about all these reactions is available from the experimental data. The stabilizer S removes P. A stabilizer is defined as effective if it suppresses the autocatalytic decomposition reaction by P. The self-decomposition reactions of NC cannot be prevented by a stabilizer.

Extended reaction scheme I (RS I-E)

$NC \xrightarrow{k_{NC,T}} P_T+R–NC$	self-decomposition by thermolysis
$NC \xrightarrow{k_{NC,H}} P_H+R–NC$	self-decomposition by hydrolysis
$NC+P_T \xrightarrow{k_{NCauto,T}} 2P_T+R–NC$	autocatalytic decomposition by P_T
$NC+P_H \xrightarrow{k_{NCauto,H}} 2P_H+R–NC$	autocatalytic decomposition by P_H
$S+P_T \xrightarrow{k_{S,T}} P–S+P_R$	stabilizing reaction
$S+P_H \xrightarrow{k_{S,H}} P–S+P_R$	stabilizing reaction

Reduced reaction scheme I (RS I)

$NC \xrightarrow{k_{NC}} P+R–NC$	combined self-decomposition
$NC+P \xrightarrow{k_{NCauto}} 2P+R–NC$	autocatalytic decomposition
$S+P \xrightarrow{k_S} P–S+P_R$	stabilizing reaction

The reaction rate equation system of RS I, Eq.(1), contains the following rate equations.

$$\left.\begin{aligned} \frac{dx_{NC}}{dt} &= -k_{NC}x_{NC} - k_{NCauto}x_{NC}x_P \qquad k_{NC} = k_{NC,T} + k_{NC,H} \\ \frac{dx_P}{dt} &= +k_{NC}x_{NC} + k_{NCauto}x_{NC}x_P - k_{DPA}x_{DPA}x_P \\ \frac{dx_{DPA}}{dt} &= -k_{DPA}x_{DPA}x_P \end{aligned}\right\} \quad (1)$$

The two decomposition reactions of NC are represented in sum by k_{NC}. All concentrations are normalized with the initial concentration NC(0) of the $CONO_2$ groups, Eq. (2), and the units mol reactant per mol $CONO_2$ group result in dimensionless quantities $x_i(t)$.

$$x_{\text{Reactant}}(t)=\text{Reactant}(t)/\text{NC}(0) \quad (2)$$

All reaction rate constants then have the dimension 1/time and can be used directly to establish reactivities.

To get values for the reaction rate constants first Eq. (1) was numerically integrated by a Runge–Kutta procedure suitable for coupled differential equations with estimated start values for the reaction rate constants. The resulting integrated data at the measurement times were then used in a non-linear parameter calculation procedure to get improved values for the reaction rate constants by comparing the Runge–Kutta values to the experimental data and by the calculation of the changes in the reaction rate constant values to get a fit with a lower standard deviation. With these new reaction rate constant values the next Runge–Kutta integration was performed, then again the non-linear parameter calculation. In this manner it was proceeded until the change in the values of the reaction rate constants was too small to give a further improvement of the fit.

Because the stabilizer DPA is very effective, the autocatalytic reaction is suppressed successfully and no information is available from measured data during the stabilizing period, see also section 'Modelling including the consecutive DPA products'. Because it cannot be excluded completely that some of the P does react with NC, the autocatalytic reaction is included in the calculation by setting k_{NCauto} to a fixed value of 10 times that of k_{NC}. The initial values of the reactants are all defined by the analytically determined values, except for x_{P}. The decomposition reaction of NC is always going on, so that x_{P} must have a value not equal to zero. From measurements of the NO_X release of NC by the NO-chemiluminescence technique, a value for $x_{\text{P}}(0)$ between 0.0005 and 0.00075 mol (mol $CONO_2$)$^{-1}$ was estimated, see the discussion in [4]. With Eq. (1), two reaction rate constants are now determinable, k_{NC} and k_{DPA}. Table 1 lists their values at the storage temperatures between 65 and 90°C. Figures 5 and 6 show their Arrhenius plots.

Table 1 Reaction rate constants k_{NC} and k_{DPA} according to the reaction rate equation system of RS I, Eq. (1), using $k_{\text{NCauto}}=10k_{\text{NC}}$ and $x_{\text{P}}(0)=0.00075$ mol (mol $CONO_2$)$^{-1}$

T/°C	k_{NC}/d^{-1}	k_{DPA}/d^{-1}	Correl. coeff.
65	3.98 E-5	24.7	0.991
70	7.92 E-5	40.2	0.994
75	1.62 E-4	234	0.995
80	3.04 E-4	310	0.987
85	7.90 E-4	206	0.996
90	1.31 E-3	807	0.997
E_a/kJ mol^{-1}	146±5	132±28	
lg(Z/d^{-1})	18.1±0.7	22±4	
Correl. coeff.	0.998	0.923	

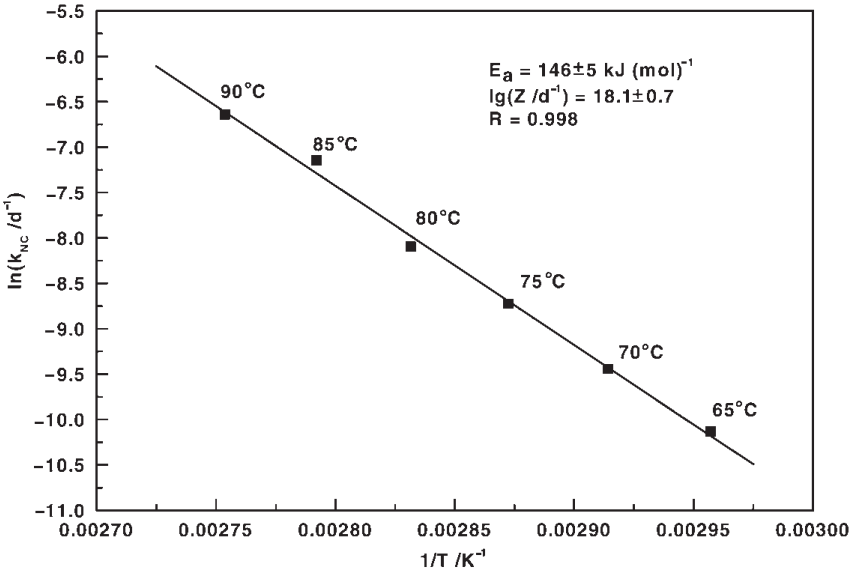

Fig. 5 Arrhenius plot of the reaction rate constant k_{NC} determined according to Eq. (1) using k_{NCauto}=10 k_{NC} and $x_P(0)$=0.00075 mol (mol $CONO_2$)$^{-1}$

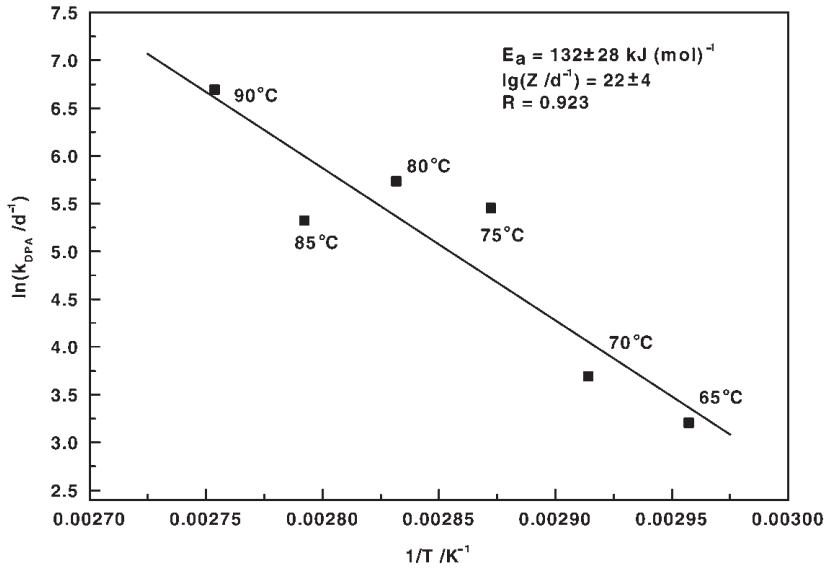

Fig. 6 Arrhenius plot of the reaction rate constant k_{DPA} determined according to Eq. (1) using k_{NCauto}=10 k_{NC} and $x_P(0)$=0.00075 mol (mol $CONO_2$)$^{-1}$

The value of E_a for k_{NC} lies with 146±5 kJ mol^{-1} between the two values of thermolysis and hydrolysis of the $CONO_2$ group given above. This suggests that both mechanisms are active in this case. The activation energy determined from values of k_{DPA} is 132±28 kJ mol^{-1}, which is in the range of the resonance energy of the aromatic benzene system of DPA. For the nitration process the aromatic resonance is disturbed and the transition state for the nitration lies energetically above the initial state by the resonance energy.

Modelling including the consecutive DPA products

The next step in modelling includes the mono-nitrated DPAs and the N–NO–DPA. The reaction scheme is given below as RS III. RS II is described in [4] but is not essential for the matter discussed here. RS III contains three parallel reactions of DPA to the first-step products of DPA. It is known that N–NO–DPA can react back to DPA, especially at higher temperatures, see for example reference [5]. This reaction is also included. The three first-step products react to form further consecutive products, which must not be specified on this modelling level. The reaction rate equation system of RS III is shown in Eq. (3).

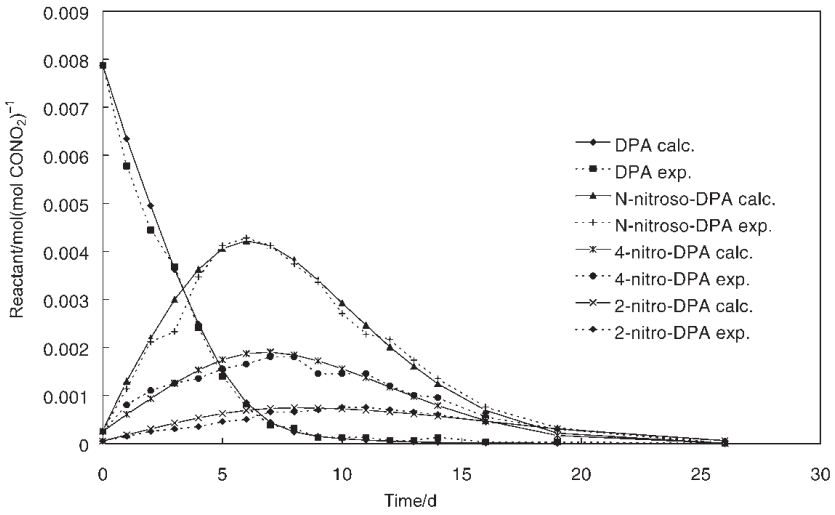

Fig. 7 Experimental and calculated concentrations at 90°C according to the reaction rate equation system of RS III with $x_P(0)$=0.0005 mol (mol $CONO_2$)$^{-1}$

Reaction scheme III (RS III)

$$NC \xrightarrow{k_{NC}} P+R$$

$$NC+P \xrightarrow{k_{NCauto}} 2P+R$$

$$\text{DPA+P} \xrightarrow{k_{NNO}} \text{N–NO–DPA}$$

$$\text{DPA+P} \xrightarrow{k_{4N}} \text{4-nitro-DPA}$$

$$\text{DPA+P} \xrightarrow{k_{2N}} \text{2-nitro-DPA}$$

$$\text{N–NO–DPA} \xrightarrow{k_{DPNNO}} \text{DPA+P}$$

$$\text{N–NO–DPA+P} \xrightarrow{k_{NNO^-}} \text{DPA}_{NNO^-}$$

$$\text{4-nitro-DPA+P} \xrightarrow{k_{4N^-}} \text{DPA}_{4N^-}$$

$$\text{2-nitro-DPA+P} \xrightarrow{k_{2N^-}} \text{DPA}_{2N^-}$$

Reaction rate equation system of RS III

$$\left.\begin{aligned}
\frac{dx_{NC}}{dt} &= -k_{NC}x_{NC} - k_{NCauto}x_{NC}x_p \\
\frac{dx_P}{dt} &= k_{NC} + x_{NC} + k_{NCauto}x_{NC}x_P + k_{DPNNO}x_{NNO} - (k_{NNO} + k_{4N} + k_{2N})x_P x_{DPA} \\
&\quad -(k_{NNO^-}x_{NNO} + k_{4N^-}x_{4N} + k_{2N^-}x_{2N})x_P \\
\frac{dx_{DPA}}{dt} &= k_{DPNNO}x_{NNO} - (k_{NNO} + k_{4N} + k_{2N})x_P x_{DPA} \\
\frac{dx_{NNO}}{dt} &= k_{NNO}x_P x_{DPA} - k_{NNO^-}x_P x_{NNO} - k_{DPNNO}x_{NNO} \\
\frac{dx_{4N}}{dt} &= k_{4N}x_P x_{DPA} - k_{4N^-}x_P x_{4N} \\
\frac{dx_{2N}}{dt} &= k_{2N}x_P x_{DPA} - k_{2N^-}x_P x_{2N}
\end{aligned}\right\} \quad (3)$$

Table 2 lists the values of the eight reaction rate constants of Eq. (3), as functions of the initial concentration of $x_P(0)$, obtained in the same way as described with Eq. (1), k_{NCauto} was set to 10 k_{NC}. There is some influence on the values by $x_P(0)$. The correlation coefficient increases with increasing $x_P(0)$. In Fig. 7 the good description of the experimental data (dotted lines) by the modelling (full lines) can be seen. About the way of determining the two fit-quality parameters standard deviation and correlation coefficient see the appendix.

Table 3 shows the influence of k_{NCauto} on the values of the other reaction rate constants, here shown relative to the values at k_{NCauto}=0. The best fit is obtained with k_{NCauto}=0, it has the highest correlation coefficient and the lowest standard deviation σ. The values of the reaction rate constants and of the two fit-quality indicators are similar up to k_{NCauto}=10k_{NC}. Then the deviations get significantly large. The conclusion

is that there is no information about the autocatalytic decomposition reaction of the NC in the measured data.

Table 2 Reaction rate constants in d^{-1} at 90°C according to the reaction rate equation system of RS III at different initial concentrations of $x_P(0)$ and with $k_{NCauto}=10k_{NC}$. The correlation coefficient and the standard deviation σ are for the total fit

Rate constant	k_X in d^{-1} at $x_P(0)$ in mol (mol $CONO_2$)$^{-1}$		
	0.0	0.0005	0.00075
k_{NC}	0.00173	0.00159	0.00155
k_{NNO}	340.8	300.1	258.6
k_{4N}	104.3	98.3	88.9
k_{2N}	44.9	35.7	32.5
k_{DPNNO}	0.089	0.0718	0.0513
k_{NNO^-}	20.8	25.75	27.31
k_{4N^-}	22.1	26.1	25.0
k_{2N^-}	9.66	10.43	9.79
Correl. coeff.	0.9916	0.9945	0.9952
St. dev. σ	2.07 E-4	1.67 E-4	1.56 E-4

Table 3 Reaction rate constants relative to the values with $k_{NCauto}=0$ at 90°C according to RS III at different values for k_{NCauto} and with $x_P(0)=0.0005$ mol (mol $CONO_2$)$^{-1}$. The correlation coefficient and the standard deviation σ are for the total fit

Rate const.	$k_{NCauto}=nk_{NC}$					
	0	1	10	50	100	300
k_{NC}	1	0.9996	0.996	0.965	0.912	0.769
k_{NNO}	1	0.998	0.987	0.993	1.096	1.783
k_{4N}	1	0.998	0.978	0.944	0.988	1.196
k_{2N}	1	0.998	0.979	0.955	1.013	1.306
k_{DPNNO}	1	1.007	1.068	1.368	1.765	4.247
k_{NNO^-}	1	0.994	0.942	0.765	0.629	0.231
k_{4N^-}	1	0.996	0.964	0.864	0.810	0.652
k_{2N^-}	1	0.995	0.961	0.860	0.796	0.674
Corr. coeff.	0.99482	0.99481	0.99466	0.99376	0.99209	0.98206
St. dev. σ	1.640 E-4	1.642 E-4	1.666 E-4	1.800 E-4	2.025 E-4	3.043 E-4

Figures 8 and 9 show the results of the calculations with reaction scheme IV, which includes all the determined consecutive products of DPA. RS IV is discussed in detail in [4], but with modelling using $x_P(0)=0$. Here $x_P(0)=0.0005$ mol (mol $CONO_2$)$^{-1}$ was taken. The scheme has 21 reaction rate constants and again k_{NCauto} was set equal to $10k_{NC}$. For the first-step products, the modelling describes the experimen-

tal data as well as does RS III. The calculated concentration courses of the di-nitrated and tri-nitrated products show some deviation from the experimental data, caused probably by the decreasing particle balance with regard to DPA. The total correlation coefficient of the parameter calculation is with 0.993 still high.

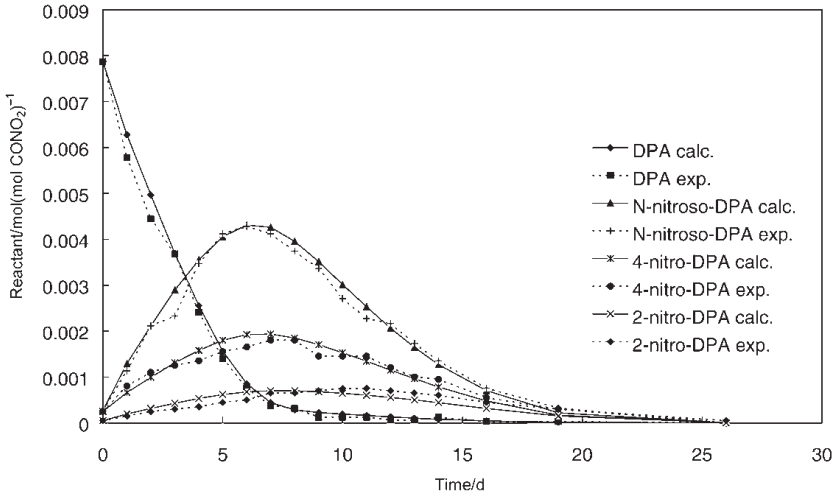

Fig. 8 Experimental and calculated concentrations at 90°C according to the reaction rate equation system of RS IV [4] with $x_P(0)$=0.0005 mol (mol $CONO_2$)$^{-1}$, part 1

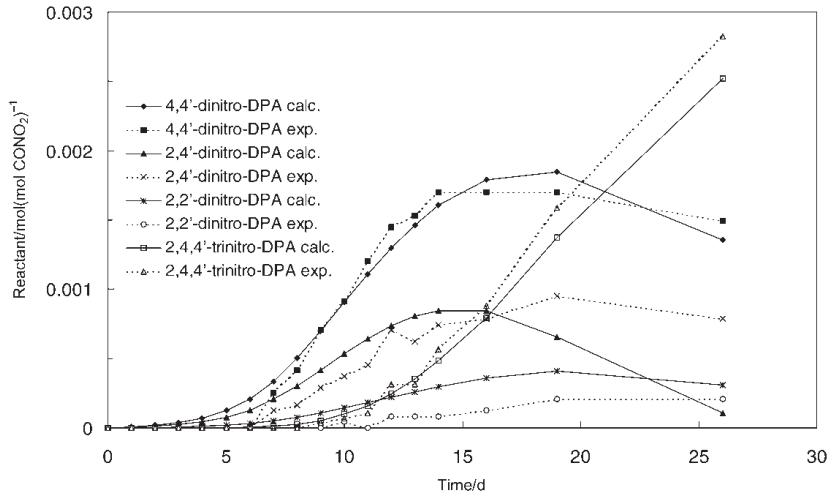

Fig. 9 Experimental and calculated concentrations at 90°C according to the reaction rate equation system of RS IV [4] with $x_P(0)$=0.0005 mol (mol $CONO_2$)$^{-1}$, part 2

Discussion

Simplification of reaction scheme III to reaction scheme III–V

In the literature, some modelling of the concentration courses of DPA and its consecutive products was reported earlier [6, 7]. In [6], no comparison with experimental data was made and the reaction scheme used was very simplified and only N–NO–DPA was included in the modelling. The authors of [7] used the same mechanistic concept as in [6], see the next section. In both cases, the kinetic steady-state approximation was applied for the concentration of P. This simplifies the resulting reaction schemes considerably. The schemes then contain only reactions of first-order or pseudo-first-order. The application of this approximation in RS III is shown below. RS III converts to the simplified reaction scheme RS III–V. The constant concentration of P is multiplied with the k_i of RS III to give the new reaction rate constants of RS III–V. The reaction rate equation system is shown in Eq. (4). It can be integrated analytically and the results for the four reactants are given below in Eq. (5) to Eq. (8). In RS III–V, parallel reactions to the first-step products of DPA are considered also.

Reaction scheme III–V (RS III–V)

$$\text{DPA+P} \xrightarrow{k_{NNO}} \text{N–NO–DPA}$$

$$\text{DPA+P} \xrightarrow{k_{4N}} \text{4-nitro-DPA}$$

$$\text{DPA+P} \xrightarrow{k_{2N}} \text{2-nitro-DPA}$$

$$\text{N–NO–DPA+P} \xrightarrow{k_{NNO^-}} \text{DPA}_{NNO^-}$$

$$\text{4-nitro-DPA+P} \xrightarrow{k_{4N^-}} \text{DPA}_{4N^-}$$

$$\text{2-nitro-DPA+P} \xrightarrow{k_{2N^-}} \text{DPA}_{2N^-}$$

Reaction rate equation system of RS III–V

$$\left.\begin{aligned}
\frac{dx_{DPA}}{dt} &= -(\bar{k}_{NNO}+\bar{k}_{4N}+\bar{k}_{2N})x_{DPA} \\
\frac{dx_{NNO}}{dt} &= \bar{k}_{NNO}x_{DPA}-\bar{k}_{NNO^-}x_{NNO} \qquad \text{with } \bar{k}_i = k_i x_P \\
\frac{dx_{4N}}{dt} &= \bar{k}_{4N}x_{DPA}-\bar{k}_{4N^-}x_{4N} \\
\frac{dx_{2N}}{dt} &= \bar{k}_{2N}x_{DPA}-\bar{k}_{2N^-}x_{2N}
\end{aligned}\right\} \quad (4)$$

Solution of the reaction scheme RS III–V, with $k_D = \bar{k}_{NNO}+\bar{k}_{4N}+\bar{k}_{2N}$

$$x_{DPA}(t) = x_{DPA}(0)\exp(-k_D t) \quad (5)$$

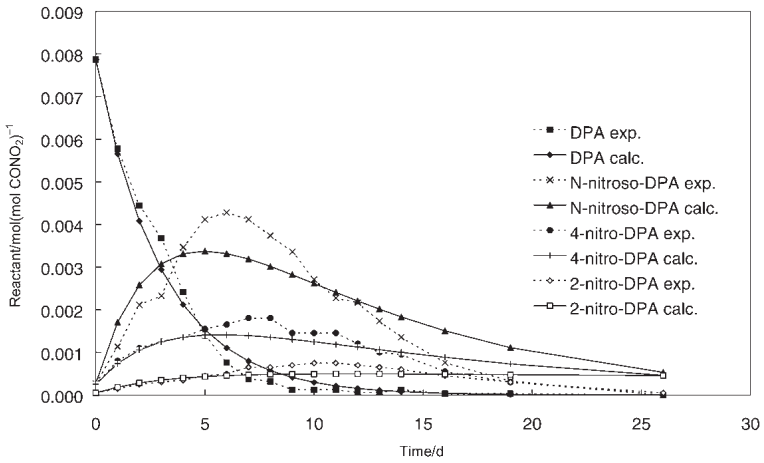

Fig. 10 Experimental data and calculated concentrations at 90°C according to the simplified reaction rate equation system RS III–V with $x_P(t)$=constant

$$x_{NNO}(t)=x_{NNO}(0)\exp(-\bar{k}_{NNO^-}t)+\frac{x_{DPA}(0)\bar{k}_{NNO}\{\exp(-\bar{k}_{NNO^-}t)-\exp(-k_D t)\}}{k_D-\bar{k}_{NNO^-}} \quad (6)$$

$$x_{4N}(t)=x_{4N}(0)\exp(-\bar{k}_{4N^-}t)+\frac{x_{DPA}(0)\bar{k}_{4N}\{\exp(-\bar{k}_{4N^-}t)-\exp(-k_D t)\}}{k_D-\bar{k}_{4N^-}} \quad (7)$$

$$x_{2N}(t)=x_{2N}(0)\exp(-\bar{k}_{2N^-}t)+\frac{x_{DPA}(0)\bar{k}_{2N}\{\exp(-\bar{k}_{2N^-}t)-\exp(-k_D t)\}}{k_D-\bar{k}_{2N^-}} \quad (8)$$

Table 4 lists the values of the reaction rate constants obtained with RS III–V, and Fig. 10 shows the comparison between the calculated and experimental data. Qualitatively the calculation is in fair agreement with the experiment, but quantitatively the description is not satisfying.

Table 4 Reaction rate constants in d^{-1} according to RS III–V at 90°C with $x_P(t)$=constant. The correlation coefficient and the standard deviation σ are for the total fit

$\bar{k}_{NNO}$	$\bar{k}_{4N}$	$\bar{k}_{2N}$	$\bar{k}_{NNO^-}$	$\bar{k}_{4N^-}$	$\bar{k}_{2N^-}$	St. dev. σ	Corr. coeff.
0.231	0.078	0.021	0.107	0.067	0.0072	3.69 E-4	0.9721

N–NO–DPA as key intermediate in the formation of the mono-nitrated DPA products

The modelling in [7] was done according to the reaction scheme RS NNO–MN, with the assumption of a consecutive reaction course first from DPA to N–NO–DPA and

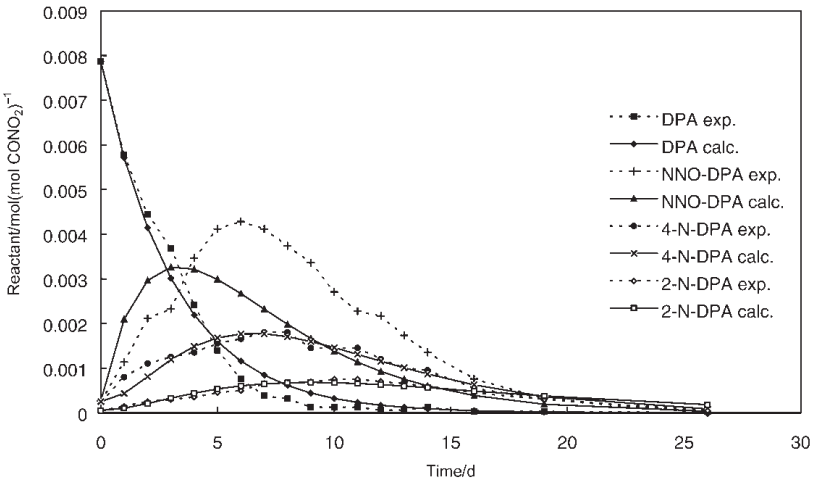

Fig. 11 Experimental data and calculated concentrations according to the simplified reaction scheme RS NNO–NM with $x_P(t)$=constant, simulating the concentration course of N-NO-DPA

then from N–NO–DPA to the two mono-nitrated DPAs, in contrast to the modelling used in RS III, RS IV and RS III–V.

Reaction scheme RS NNO-MN

$$\text{DPA+P} \xrightarrow{k_{NNO}} \text{N–NO–DPA}$$

$$\text{N–NO–DPA+P} \xrightarrow{k_{4NNO}} \text{4-nitro-DPA+P}'$$

$$\text{N–NO–DPA+P} \xrightarrow{k_{2NNO}} \text{2-nitro-DPA+P}'$$

$$\text{N–NO–DPA+P} \xrightarrow{k_{NNO^-}} \text{DPA}_{NNO^-}$$

$$\text{4-nitro-DPA+P} \xrightarrow{k_{4N^-}} \text{DPA}_{4N^-}$$

$$\text{2-nitro-DPA+P} \xrightarrow{k_{2N^-}} \text{DPA}_{2N^-}$$

The authors in [7] had experimental data for DPA and the two mono-nitrated DPAs, but not for N–NO–DPA. They simulated the concentration course of this key intermediate. In that way they achieved a good description of the concentration courses of DPA and of the two mono-nitrated DPAs, because the algorithm simulates the concentration course of N–NO–DPA in such a way, to get a good description of the concentration courses of the mono-nitrated DPAs. This mechanism of a consecutive course from DPA to N–NO–DPA to the two mono-nitrated DPAs is therefore not confirmed by this type of modelling. Further the mono-nitrated DPA products should appear with an induction period and they should show an inflexion point at the same time as the maximum of the N–NO–DPA curve occurs. Because N–NO–DPA is

formed in relatively high concentrations, its reactivity is not high and an induction period should be clearly recognizable, but this is not the case in the experimental data. Figure 11 shows the description of the experimental data of this work according to the mechanism and modelling used in [7]. The simulated concentration course of N–NO–DPA deviates strongly from the experimental one. The induction periods of the calculated concentration courses of the mono-nitro DPAs can be seen especially for 4-NO_2–DPA.

Relative reactivities of the consecutive products

The establishment of the relative reactivities of the DPA products is shown, as an example, with the results of the RS III–V modelling, Table 5. Analogous calculations were performed with the reaction rate constants of RS III and RS IV. The absolute reactivity EA_X is set proportional to the sum of the reaction rate constants, which this compound shows in its reactions to other products. The relative reactivities ER_X with regard to DPA are obtained by dividing the values of EA_X with EA_{DPA}.

Table 5 Example of how to establish the absolute and relative reactivities of DPA and of its first-step products

$EA_{DPA}=C(\bar{k}_{NNO}+\bar{k}_{4N}+\bar{k}_{2N})=C0.33$	$ER_{DPA}=EA_{DPA}/EA_{DPA}=1$
$EA_{NNO}=C(\bar{k}_{NNO^-})=C0.107$	$ER_{NNO}=EA_{NNO}/EA_{DPA}=0.32$
$EA_{4N}=C(\bar{k}_{4N^-})=C0.067$	$ER_{4N}=EA_{4N}/EA_{DPA}=0.20$
$EA_{2N}=C(\bar{k}_{2N^-})=C0.0072$	$ER_{2N}=EA_{2N}/EA_{DPA}=0.022$

Table 6 Values of the relative stabilizing effectivities or reactivities ER_X obtained with the reaction rate constants of RS III, RS IV and RS III–V, as well as from [8], [9] and [10]. RT means room temperature

	RS III 90°C	RS IV 90°C	RS III–V 90°C	From [8] RT	From [9] RT	From [10] RT
DPA	1.0	1.0	1.0	1.0	1.0	1.0
N-nitroso-DPA	0.043	0.041	0.32	0.32	0.7	–
4-mono-nitro-DPA	0.045	0.074	0.20	0.38	–	–
2-mono-nitro-DPA	0.020	0.055	0.0022	0.13	0.7	0.86
4,4'-di-nitro-DPA	–	0.008	–	–	–	–
2,2'-di-nitro-DPA	–	0.004	–	–	–	–
2,4'-di-nitro-DPA	–	0.016	–	–	–	–
2,4,4'-tri-nitro-DPA	–	8 E–5	–	–	–	–

In Table 6, the relative reactivities, according to RS III, RS IV, RS III–V and values published in the literature, are compiled. These literature data have been determined at room temperature and in the following ways. In [9], the mass increase was used when DPA, N–NO–DPA and 2-NO_2–DPA, each alone, were exposed to a dry NO_2 gas stream.

In [10], exposure to a dry NO_2/N_2 gas stream was used, but here the decrease of NO_2 was measured by the NO-chemiluminescence technique. With each stabilizer, a NC model formulation was made in [10]. A distinction between NO_2 reacted with the stabilizer and with the matrix of the NC formulation was not made. In both cases, only a summarizing information for the cause of the NO_2 depletion is obtained, because the corresponding consecutive products also bind NO_2, which results in a too high reactivity value assigned to the primary stabilizer. Further the diffusion from the gas phase into the solid phase influences the results and the dry gas flow effects the humidity in the samples. In [8], the stabilizers each alone were deposited on powdered cellulose and exposed to definite amounts of NO_2 in an air atmosphere inside a flask. Humidity was not controlled in the atmosphere and in the samples. The analyses of the stabilizer products were made by HPLC. The reactivities were obtained by comparing the reaction rate constants obtained by modelling only the decreases of each of the primary stabilizers. In contrast, the reactivities of this work were calculated from reaction rate constants determined from the situation inside a real production-scale NC formulation. NO_2 was formed by NC itself, the primary stabilizer DPA was the starting compound and the method of production was typical for such formulations. The values of RS III and RS IV can be considered, therefore, as the most appropriate ones. Differences in the ER_X of the two sets originate from the different levels of modelling of the consecutive products. The values of RS IV are the more correct ones, because more reaction channels are included. The reactivity sequence at 90°C according to RS IV is DPA>>4-NO_2–DPA>2-NO_2–DPA> N–NO–DPA.

Table 7 Reaction rate constants k_S^1 and k_S^2 obtained with the 'exponential+linear' model [11] from ageing data at 90°C and some of the times, ty_S, to reach the degree of stabilizer consumption $y_S=S_{eff}(ty_S,T)/S_{eff}(0)$

Quantity	DPA_{prim}	DPA_{eff}–RS III	DPA_{eff}–RS IV
$S_{eff}(0)$/mass%	1.24	1.244	1.245
k_S^1/d^{-1}	2.9922 E-1	2.8477 E-1	2.8456 E-1
k_S^2/mass%$(d)^{-1}$	9.5354 E-3	3.9917 E-3	8.3321 E-4
Correl. coeff.	0.995	0.996	0.996
$t_{0.5}$/d	2.23	2.40	2.43
$t_{0.1}$/d	7.0	7.8	8.0
$t_{0.05}$/d	8.7	9.9	10.4
t_0/d	12.3	15.8	21.3

Prediction of extended service time period with effective stabilizer concentrations

The multiplication of the molar related concentration of a species X, for example N–NO–DPA, with ER_{NNO} gives an effective DPA-concentration value for N–NO–DPA. The total effective DPA concentration DPA_{eff} is calculated and the model 'exponential+linear' [11] is taken to predict the service time periods. The concentration data are transformed to mass percentages always used for this purpose. The results are shown in

Table 7 for the reaction schemes RS III and RS IV. The time ty_S is the time to reach the degree of stabilizer consumption $y_S=S_{eff}(ty_S,T)/S_{eff}(0)$. The time t_0 to reach $y_S=0$ or $S_{eff}(ty_S,T)=0$ increases considerably, from 12.3 days with the primary DPA alone, to 21.3 days including all measured consecutive products. The time to 'autocatalysis', which means in this case the formation of NO_2 visible by eye (this corresponds to the autoignition state of the formulation), was found to be 34 to 35 days at 90°C.

Conclusions

Kinetic modelling of the mechanisms of stabilizer reactions in a NC formulation was performed and discussed, including the consecutive products of the stabilizer DPA. This has enabled the relative reactivities of the consecutive products on the stabilizing effect, valid inside the real NC formulation, to be established and the consecutive products to be included in a defined way in the prediction of the safe and/or reliable service time periods. Reactivities obtained by former investigators with other methods have the disadvantage of being determined in environments not comparable with the situation in the real NC formulation. Our kinetic modelling was compared with the simplified modelling, which uses the kinetic steady-state approximation for the concentration of the autocatalytic product formed by the NC decomposition. It was shown that this approximation does not give satisfactory descriptions of the experimental data. The non-simplified modelling of the concentrations of the stabilizer and its products can be used to find out the correct reaction channels and to assess reaction mechanistic ideas about the stabilizer reactions. An example for this is the mechanistic role of N–NO–DPA in the formation of the mono-nitrated DPA products.

* * *

Dr. F. Volk, ICT, has provided the concentration data of DPA and its consecutive products. Dr. N. Eisenreich, ICT, has supported the modelling.

Appendix

The fit-quality parameters correlation coefficient *KK* and standard deviation σ have been determined for the total parameter calculations according to RS I, RS III, RS IV and RS III–V. At first the sum of the squared deviations between the experimental values y_i and the values F_i, calculated by the algorithm, of the dependent variable is needed, named *FQ*, Eq. (A-1).

$$FQ=\sum_{i=1}^{N}(y_i-F_i)^2 \tag{A-1}$$

The dependent variable is here the concentrations of DPA and its consecutive products. *N* is the number of measured data pairs and *m* is the number of parameters which are to be fitted, here the number of reaction rate constants. The standard deviation σ is calculated according to Eq. (A-2).

$$\sigma=\sqrt{\frac{FQ}{N-m}} \tag{A-2}$$

The total correlation coefficient *KK* of a parameter calculation is based on a comparison between two sums of squared deviations. One is *FQ*, the other is named *MQ*, which takes the arithmetic mean of the data values y_i as reference. Equation (A-3) shows the determination of *MQ*.

$$\left.\begin{aligned} MQ &= \sum_{i=1}^{N} (y_i - My)^2 \\ \text{with } My &= \frac{\sum_{i=1}^{N} y_i}{N} \end{aligned}\right\} \qquad \text{(A-3)}$$

With Eq. (A-4) the correlation coefficient *KK* can now be determined.

$$KK = \sqrt{1 - \frac{FQ}{MQ}} \qquad \text{(A-4)}$$

References

1 M. A. Hiskey, K. R. Brower and L. C. Oxley, J. Phys. Chem., 95 (1991) 3955.
2 B. Lurie, Z. Valishina and V. Malchevski, Proc. 24th Internat. Annual Conference of ICT, June 29 to July 2, 1993, p. 57-1.
3 M. A. Bohn, Thermochim. Acta, 337 (1999) 121.
4 M. A. Bohn and N. Eisenreich, Propell. Explos. Pyrotech., 22 (1997) 125.
5 P. Welzel, Chem. Ber., 104 (1971) 808.
6 B. Zeller and J. P. Lucette, Proc. 'Internat. Symp. on Gun Propellants', October 15 to 19, 1973. Ed.: US Army Picatinny Arsenal, Dover, USA, New Jersey 1973.
7 A. Bergens and B. Nygard, Proc. 9th Symp. on 'Chemical Problems Connected with the Stability of Explosives', Ed.: J. Hansson, Sweden, Sundbyberg 1993, p. 161.
8 L. S. Loussier, H. Gagnon and M. A. Bohn, Propell. Explos. Pyrotech., 25 (2000) 117.
9 A. Alm, Proc. 1st Symp. on 'Chemical Problems Connected with the Stability of Explosives', Ed.: J. Hansson, Sweden, Stockholm 1968, p. 162.
10 I. G. Wallace and S. Westlake, Proc. 7th Symp. on 'Chemical Problems Connected with the Stability of Explosives', Ed.: J. Hansson, Sweden, Sundbyberg 1985, p. 162.
11 M. A. Bohn, Propell. Explos. Pyrotech., 19 (1994) 266.